Available online at www.sciencedirect.com

Journal of Applied Research and Technology

Journal of Applied Research and Technology 13 (2015) 537–542

www.jart.ccadet.unam.mx

Original

Reversible holography and optical phase conjugation for image formation/correction using highly efficient organic photorefractive polymers

José-Luis Maldonado [a,*], Víctor-Manuel Herrera-Ambriz [a], Mario Rodríguez [a], Gabriel Ramos-Ortíz [a], Marco-Antonio Meneses-Nava [a], Oracio Barbosa-García [a], Rosa Santillan [b], Norberto Farfán [c]

[a] *Centro de Investigaciones en Óptica, A.P. 1-948, 37000 León, Gto., Mexico*
[b] *Departamento de Química, CINVESTAV del IPN, A.P. 14-740, 07000 México, D.F., Mexico*
[c] *Facultad de Química, Departamento de Química Orgánica UNAM, 04510 México, D.F., Mexico*

Received 19 March 2015; accepted 12 August 2015
Available online 17 November 2015

Abstract

In this work, we report the reversible reconstruction of holographic and distorted transmission images through the four wave mixing (FWM) technique and optical phase conjugation (OPC), an alternative method to adaptive optics, by using highly efficient Photorefractive (PR) polymers fabricated in our laboratories. These PR polymers are based on our synthesized nonlinear chromophore 4-[4-(diethylamino)-2 hydroxybenzylideneamino] benzonitrile (**Dc**). For the PR devices, diffraction efficiencies as high as 90% at 25 wt.% doping level of **Dc** at an external applied electric field (E_{ext}) around 56 V/μm are achieved. The reconstruction implementation is simple, of low cost, all-optical and it is capable of recovering 90% of the original images. The real-time holographic experiments were performed at E_{ext} of just 27 V/μm, which is one of the lowest reported values. Reversible holographic imaging is showed with a rise-time around 0.35 s.

Keywords: Real-time reconstructions; Photorefractive polymers; Optical phase conjugation

1. Introduction

In image formation/detection with codified information, aberration media, such as atmospheric turbulence, perturb the phase and cause intensity scintillation on the detectors. The scintillation reduces the information capacity and increases the bit error rate. Adaptive optics technology can dynamically correct the spatial aberrations in the transmitted beams, which carry the information, and significantly improve the performance (Levine et al., 1998; Li et al., 2005). A typical adaptive optics system includes a wave front sensor for measurement of the aberrations, an actuator for wave front correction, and the corresponding control electronics. Implementation of such a system is expensive and complex. Considerable research efforts have been devoted to develop real-time, low-cost adaptive optical systems, for instance, by using nonlinear optical (NLO) effects by means of the photorefractive (PR) phenomenon through optical phase conjugation (OPC) and multiple wave mixing (MWM) (Joo, Kim, Chun, Moon, & Kim, 2001; Köber, Salvador, & Meerholz, 2011; Li et al., 2005; Simonov, Larichev, Shibaev, & Stakhanov, 2001; Sun & Dalton, 2008; Winiarz & Ghebremichael, 2004). PR dynamic holographic techniques are also of interest for laser communication and information processing since fast, low-cost, and all-optical compensation of wave front distortion can be achieved without expensive actuators (deformable mirrors), sophisticated computation, and complex electronics (Günter & Huignard, 2007; Günter, 2000; Köber et al., 2011; Levine et al., 1998; Li et al., 2005; Sun & Dalton, 2008).

* Corresponding author.
E-mail address: jlmr@cio.mx (J.-L. Maldonado).
Peer Review under the responsibility of Universidad Nacional Autónoma de México.

http://dx.doi.org/10.1016/j.jart.2015.10.007

OPC is one of the most important phenomena in PR materials. Full theoretical treatment of the OPC can be found elsewhere (Yeh, 1993). Briefly, when a plane wave front passes through an inhomogeneous medium with refractive index $n(x,y,z)$, it distorts the wave front. If the wave is now reflected backwards by an ordinary mirror and again passes through the medium, the distortion of the wave front accumulates. In contrast, if the wave is reflected from a phase-conjugated mirror creating the phase-conjugated replica, distortion is canceled, and the wave front is reconstructed. Some of the potential applications include transmission of undistorted images through optical fibers (or through the atmosphere), refreshing of holograms for long-term optical storage, optical interferometry, beam cleanup, and image processing (Sun & Dalton, 2008). In a classic geometry (FWM), phase conjugation occurs when two counter propagating pump beams overlap in a PR material and create a phase-conjugated replica of a third incident beam (Sun & Dalton, 2008; Yeh, 1993).

PR compounds need to possess simultaneously photosensitivity, photoconductivity and electro-optic (EO) properties. These materials are ideal for potential applications in real-time optical processing because they provide a medium for reversible and nonlocal volume holography (Blanche et al., 2010; Günter & Huignard, 2007; Günter, 2000; Köber et al., 2011; Moon, Choi, & Kim, 2013; Sun & Dalton, 2008), for instance, recently the use of PR polymers for demonstration of holographic three-dimensional telepresence was reported (Blanche et al., 2010). The pioneer report on organic polymer-based PR composites by Ducharme, Scott, Twieg, and Moerner (1991) generated an intensive research with these materials, and in 1994 appeared the first report of nearly 100% diffraction efficiency (η) by Meerholz, Volodin, Kippelen, and Peyghambarian (1994). In these PR devices, a spatial optical excitation (interference pattern) produces, through a sensitizer, a number of mobile holes/electrons, which drift under an external applied electric field E_{ext}, and are subsequently trapped on the dark regions of the interference pattern (Oh, Lee, & Kim, 2009). The resulting space charge electric field, E_{sc}, alters the refractive index of the polymer blend through the electro-optic effect (Kukhtarev, Markov, Odulov, Soskin, & Vinetskii, 1978; Oh et al., 2009). Reorientation of the nonlinear (NL) chromophores, under the combined effects of E_{sc} and E_{ext}, leads to a modulated birefringence, further enhancing the refractive index modulation (Günter & Huignard, 2007; Günter, 2000; Sun & Dalton, 2008). The resulting index pattern has the same period as the interfering light that generates the photo-carriers, but its phase is shifted. This phase shift is an evidence of the PR effect and leads to an energy exchange between the two coherent beams that generate the light grating. For PR polymers, however, a strong external electric field is necessary for charge photogeneration, high hole/electron mobility and orientational birefringence (Maldonado et al., 2007; Ostroverkhova & Moerner, 2004; Zhao et al., 2011). Regarding this fact, in the literature, few reports of highly efficient PR polymers at fields lower than 60 V/μm are found (Hendrickx et al., 1998; Joo et al., 2001; Kippelen et al., 1998; Maldonado et al., 2009; Tay et al., 2008; Thomas et al., 2004), so, the reduction of E_{ext} values is a very important feature to take into account in the development of novel organic PR materials and for the realization of technological applications.

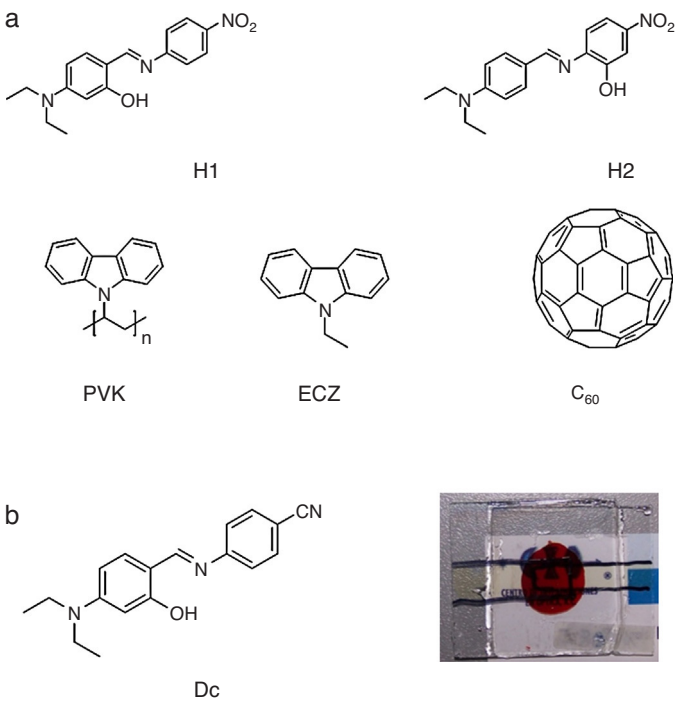

Fig. 1. (a) Molecular structure of our previously used nonlinear molecules **H1** and **H2** (Maldonado et al., 2009), the polymer matrix PVK, the plasticizer ECZ and the sensitizer fullerene C_{60}. (b) Molecular structure of the NL **Dc** chromphore used in this work and a photograph of a PR polymer device doped with **Dc**.

Optimization of the PR effect in organic materials generally involves the synthesis of *push-pull* molecules (chromophores) (Marder, Kippelen, Jen, & Peyghambarian, 1997; Moon & Kim, 2009; Würthner, Wortmann, & Meerholz, 2002) with strong linear and microscopic NLO properties, i.e., the permanent dipole moment μ, the polarizability anisotropy $\Delta\alpha$ (birefringence contribution), and the first hyperpolarizability β (EO contribution) (Marder et al., 1997; Moon & Kim, 2009). Recently, we have reported very high diffraction efficiencies at low applied electric field on PR compounds based on the dipolar arylimine chromophores **H1** and **H2** (Maldonado et al., 2009), see Figure 1, obtaining 87% and 75% at just $E_{ext} = 48$ V/μm and 32 V/μm, respectively; likewise, using the chromophore **Dc**, from the same family, diffraction efficiencies as high as 90% and 82% were achieved at just $E_{ext} = 56$ V/μm and 63 V/μm, respectively (Herrera-Ambriz et al., 2011). Our PR polymers based on **Dc** were also recently employed in a laser ultrasonic receiver (Zamiri et al., 2015) as contactless and adaptive interferometers, which are used widely for materials characterization (Davies, Edwards, Taylor, & Palmer, 1993; Zamiri et al., 2014).

In this work, by using our PR polymers based on **Dc** NL chromophore synthesized in our labs, reversible holographic transmission images and reconstruction of distorted figures by OPC under the FWM technique are reported. These reversible reconstructions were performed at one of the smallest E_{ext} values reported in the literature: 27 V/μm. Typical response time

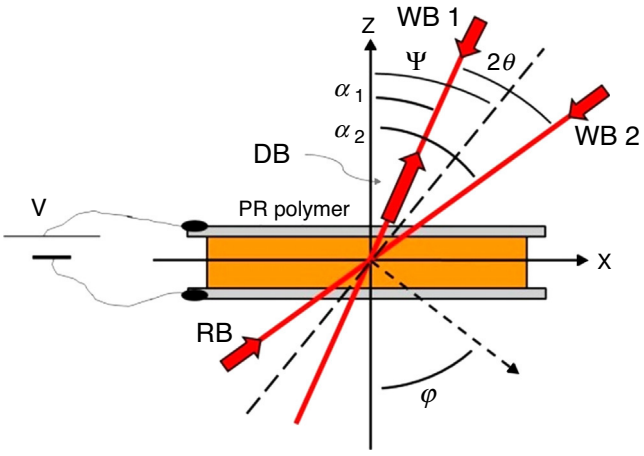

Fig. 2. Geometry used in FWM measurements, holographic imaging and image reconstruction, where WB = writing beam (object and reference beams) and RB = reading beam. RB is in the opposite direction of WB2, DB = diffracted beam (phase-conjugated signal).

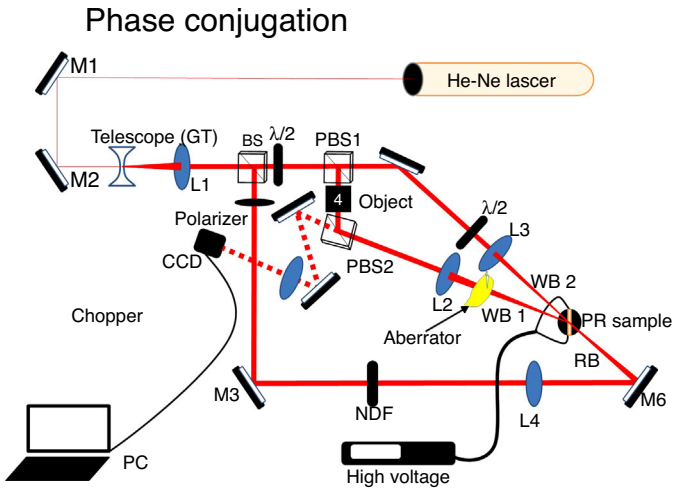

Fig. 3. Experimental setup: M = mirror, L = lens, PBS = polarizing beam splitter, BS = beam splitter, λ/2 = half wave plate, NDF = neutral density filter, PC = personal computer.

of our PR polymers is about 350 ms, which enable these reconstructions at a reasonable fast speed.

2. Materials and methods

2.1. Materials

Dc was synthesized in our laboratories according to typical synthesis procedure (Meyer, Joiner, & Stoddart, 2007) by condensation reaction between 4-aminobenzonitrile and 4-diethylaminosalicylaldehyde in methanol. Starting material and solvents were purchased from Sigma–Aldrich and all of them were used without further purification.

2.2. PR sample preparation

We made thick, solid film samples of **Dc** in combination with the widely used mixture of PVK:ECZ:C_{60}, PVK being the photoconducting polymer matrix and ECZ the plasticizer (Kippelen et al., 1998; Maldonado et al., 2009; Sun & Dalton, 2008), at 25:49:25:1 wt.%. Magnetic stirring in dichloromethane dissolved the **Dc**:PVK:ECZ constituents. The sensitizer fullerene C_{60} was previously dissolved in toluene and then mixed with the **Dc**:PVK:ECZ solution. The final mix was filtered through a 11 μm pore size paper filter. Solvent was evaporated under reduced pressure, and the mixture was subsequently dried in an oven at 60 °C, for 12 h. Next, the dried material was melted and mixed within two large glass slides. A small piece of the resulting film was cut, and melted between two ITO-coated glass slides at a temperature of about 145–160 °C. Calibrated glass spacers of thickness $d = 110$ μm were used to ensure a uniform sample thickness.

2.3. Holographic experiments

The performance of our PR polymers was tested with a tilted four wave mixing (FWM) and two beam coupling (TBC) geometries (Köber et al., 2011); details of our experimental set up can be found elsewhere (Herrera-Ambriz et al., 2011; Maldonado et al., 2009). Figure 2 shows the used geometry for the dynamic holographic experiments and OPC. The FWM experimental set up is shown in Figure 3. Briefly, our experiments were performed with a 10 mW He–Ne laser ($\lambda = 633$ nm). The writing beams (WBs) had *s*-polarization, each with power of ∼0.7 mW. They were focused on the sample, with a spot size of ∼1.5 mm; so, the recording light intensities (I) were of ∼40 mW/cm^2. The angle 2θ ($\alpha_2 - \alpha_1$) between the writing beams outside the sample was 21°, whereas the tilt angle ψ was 60°. The refractive index of the polymer composites, measured with a reflectometer (Filmetrics F20), resulted in $n = 1.58$–1.60 at 633 nm. The grating spacing under these conditions was 2.9 μm (Herrera-Ambriz et al., 2011; Maldonado et al., 2009). Measurements of the diffraction efficiency were carried out with a *p*-polarized probe/reading beam with a spot size of <1.5 mm and a power of only a thousandth (1/1000) of the power of the writing beams. In FWM geometry, it is typical to have different polarization for the writing and reading beams in order to neglect possible effects of the probe beam on the grating even when its intensity is much weaker than that of the writing beams.

For image reconstruction, holograms of two-dimensional objects (of about 5 mm in size) on a slide were employed (before PSB2 in Figure 3). In dynamic holography, a hologram can be stored, or erased, without the need of a development step. It can be used in an unlimited number of write–erase cycles, and can virtually display information in real time. In our case, holographic images were acquired by using the Bragg diffraction of a reading beam (diffracted phase-conjugated signal). To have control over the beam size (about 8 mm in diameter) a beam expander (Galilean telescope) was implemented. In the formation of dynamic holographic images, the probe beam was *p*-polarized, and was sent into the PR polymer with a spot size of ∼2 mm in the vicinity of the sample. After reconstruction, the holographic images were sent into a small,

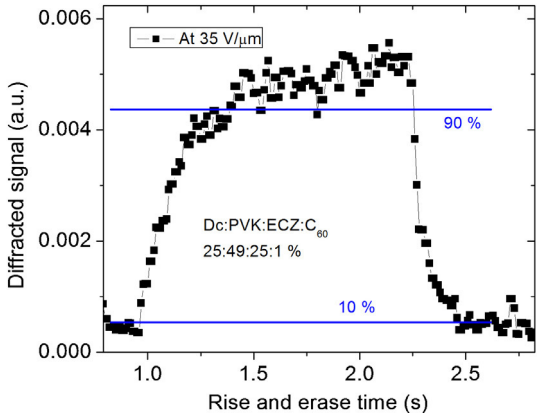

Fig. 4. Rise time is $\tau \sim 350$ ms (dynamic diffracted signal) for PR polymers **Dc**:PVK:ECZ:C_{60} (25:49:25:1 wt.%) at E_{ext} of 35 V/μm. Faster decay (erase) time is observed.

simple and nonexpensive CCD camera eliminating with this the need for electronic processing.

Once image reconstruction (without aberration medium) was proved, for OPC demonstration, the image deformation was achieved by an aberration medium placed between L2 and the PR sample, to intentionally distort the beam, as shown in Figure 3. Here, a glass Petri dish was used to distort the WB1 image information. The phase-conjugated image was achieved with the diffracted beam (DB) in the opposite direction of WB1. DB crosses the aberration medium again and generates the corrected image detected with the cheap and small CCD camera.

3. Results and discussion

In Table 1, some NL parameters of Dc and the main holographic values (Herrera-Ambriz et al., 2011) of our PR polymers used in this work are summarized.

Rise time (τ) for our PR polymers based on **Dc** chromophore is shown in Figure 4: from 10% to 90% of this diffraction efficiency, the τ value is about 350 ms, which is a very acceptable time for holographic and optical phase conjugation re-constructions because, in some reports, this time is of several seconds (Joo et al., 2001; Simonov et al., 2001; Winiarz & Ghebremichael, 2004; Winiarz, 2007). Even shorter times were recorded for the erasure process. These rise and erase times were determined as follows: when one of the WB is illuminating the PR sample with the applied external electric field "on", the second WB is sent to the PR sample and the evolution of the diffracted signal is monitored in time. Then, the same WB is blocked and the drop of the diffraction is obtained.

Figures 5 and 6 show image photographs of two objects (military target and Leon soccer club logo: real images through the PR sample), their holographic reconstructed photos, the distorted images (by using a glass Petri dish) and their restored phase-conjugated images. It can be seen that the images are severely distorted and cannot be recognized at all unless the OPC process is used to retrieve them. Resolution of the images was limited by the CCD pixel size. Images were formed in less than ~0.35 s, which is a reasonably short period of time (Joo et al., 2001; Simonov et al., 2001; Winiarz & Ghebremichael, 2004; Winiarz, 2007). Also, these experiments were performed at E_{ext} of just 27 V/μm, which is one of the lowest fields found in the literature (Herrera-Ambriz et al., 2011; Joo et al., 2001; Köber et al., 2011; Li et al., 2005; Maldonado et al., 2009; Winiarz & Ghebremichael, 2004; Winiarz, 2007).

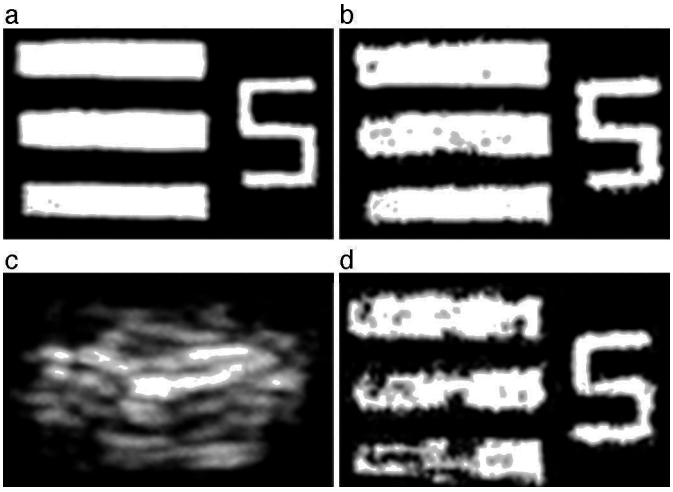

Fig. 5. Photographs of (a) original image of a military target through the PR sample, (b) transmission holographic reconstructed image (without aberration medium), (c) transmitted distorted image by using a glass Petri dish and (d) restored phase-conjugated image.

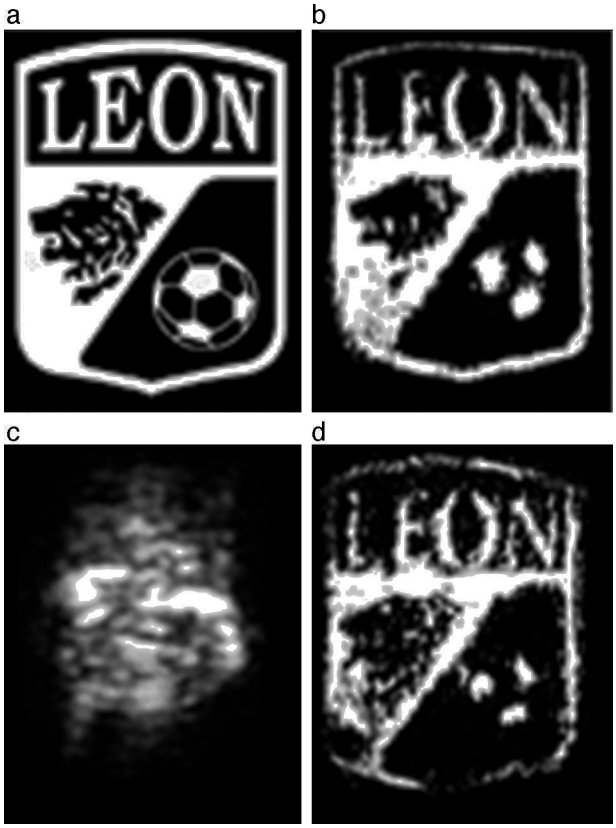

Fig. 6. Photographs of (a) original image of Leon soccer club logo through the PR sample, (b) holographic reconstructed image, (c) distorted image by using a glass Petri dish and (d) restored phase-conjugated image.

Table 1
Computed β and μ for **Dc** (in chloroform). Experimental value of the product $\beta\mu$ (through EFISH technique) = 320 esu D. Our PR composites and their measured values for the holographic parameters are shown. A He–Ne laser (633 nm) was used. Sample thickness d = 110 μm; absorption coefficient α was at 633 nm (Herrera-Ambriz et al., 2011).

PR composite 25:49:25:1 wt.%	β (10^{-30} esu)	μ (D)	λ^{a}_{max} (nm)	α (cm^{-1})	η_{max}, % (E_{ext}, V/μm)	Δn, $\times 10^{-3}$ (E_{ext}, V/μm)
Dc:PVK:ECZ:C60	15.8	9.08	401	~35	90 (56)	2.22 (63)

From Figures 5 and 6 (a), (b) and (d), one can visually see that the distorted images were acceptably corrected in the sense that they are clearly recognized from the originals (a). The two-dimensional cross-correlation is a widely used technique for recognizing patterns in images and determines the percentage similarity of two pictures (Baxes, 1994). This technique allows a sub-picture $w(x, y)$ of size $K \times L$ to be localized within an image $f(x, y)$ of greater size $M \times N$, where $K,L \leq M \leq N$. Here, the correlation to compare images was performed in Matlab using the equation:

$$r = \frac{\sum_m \sum_n (I_{mn} - \bar{I})(J_{mn} - \bar{J})}{\sqrt{\left(\sum_m \sum_n (I_{mn} - \bar{I})^2\right)\left(\sum_m \sum_n (J_{mn} - \bar{J})^2\right)}}$$

where I is the original holographic image, J is the distorted or the reconstructed object, and $\bar{I}$ and $\bar{J}$ are the average values of the image pixels.

Image in Figure 5(c) is distorted more than 54% and the restored image, Figure 5(d), has 89% of reconstruction in comparison with the holographic image (Fig. 5b). For the case of Leon soccer team logo, it is distorted 56% and it is reconstructed 79% with respect to Figure 6(b).

Chemical-structural stability of our samples is of several months and when there exists some damage, it is just enough to heat the samples above 100 °C to recover their optical quality (see photo in Figure 1b) for some more days or even weeks.

4. Conclusions

In this work, by using highly efficient organic photorefractive polymers and through the FWM technique and optical phase conjugation, we corrected images that present a high degree of aberration. Images were distorted by ~55% and were recovered ~90% with respect to the original ones. We were able to correct images almost unrecognizable to the human eye. The rise time of our PR polymers was very acceptable: ~350 ms. In order to perform these reconstructions, the external applied field E_{ext} was one of the lowest found in the literature: 27 V/μm. This all-optical set up based on NLO effects, through the PR phenomenon, for image cleanup is simple and of low cost.

Conflict of interest

The authors have no conflicts of interest to declare.

Acknowledgments

This work was supported by CONACyT project 55250. Authors also thank M. Olmos and Diego Torres A. for their technical assistance.

References

Baxes, G. A. (1994). *Digital image processing: Principles and applications*. USA: John Wiley & Sons, Inc.

Blanche, P. A., Bablumian, A., Voorakaranam, R., Christenson, C., Lin, W., Gu, T., et al. (2010). Holographic three-dimensional telepresence using large-area photorefractive polymer. *Nature*, *468*(7320), 80–83.

Davies, S. J., Edwards, C., Taylor, G. S., & Palmer, S. B. (1993). Laser-generated ultrasound: Its properties, mechanisms and multifarious applications. *Journal of Physics D: Applied Physics*, *26*(3), 329–348.

Ducharme, S., Scott, J. C., Twieg, R. J., & Moerner, W. E. (1991). Observation of the photorefractive effect in a polymer. *Physical Review Letters*, *66*(14), 1846–1849.

Günter, P. (Ed.). (2000). *Nonlinear optical effects and materials*. Berlin, Germany: Springer-Verlag.

Günter, P., & Huignard, J.-P. (Eds.). (2007). *Photorefractive materials and their applications 2*. New York, USA: Springer.

Hendrickx, E., Herlocker, J., Maldonado, J. L., Marder, S. R., Kippelen, B., Persoons, A., et al. (1998). Thermally stable high-gain photorefractive polymer composites based on a tri-functional chromophore. *Applied Physics Letters*, *72*, 1679–1681.

Herrera-Ambriz, V. M., Maldonado, J. L., Rodríguez, M., Castro-Beltrán, R., Ramos-Ortíz, G., Magaña-Vergara, N. E., et al. (2011). Highly efficient photorefractive organic polymers based on benzonitrile shiff bases nonlinear chromophores. *Journal of Physical Chemistry C*, *115*(48), 23955–23963.

Joo, W. J., Kim, N. J., Chun, H., Moon, I. K., & Kim, N. (2001). Polymeric photorefractive composite for holographic applications. *Polymer*, *42*(24), 9863–9866.

Kippelen, B., Marder, S. R., Hendrickx, E., Maldonado, J. L., Guillemet, G., Volodin, B. L., et al. (1998). Infrared photorefractive polymers and their applications for imaging. *Science*, *279*(5347), 54–57.

Köber, S., Salvador, M., & Meerholz, K. (2011). Organic photorefractive materials and applications. *Advanced Materials*, *23*(41), 4725–4763.

Kukhtarev, N. V., Markov, V. B., Odulov, S. G., Soskin, M. S., & Vinetskii, V. L. (1978). Holographic storage in electrooptic crystals. I. Steady state. *Ferroelectrics*, *22*(1), 949–960.

Levine, B. M., Martinsen, E. A., Wirth, A., Jankevics, A., Toledo-Quinones, M., Landers, F., et al. (1998). Horizontal line-of-sight turbulence over near-ground paths and implications for adaptive optics corrections in laser communications. *Applied Optics*, *37*(21), 4553–4560.

Li, G., Eralp, M., Thomas, J., Tay, S., Schülzgen, A., Norwood, R. A., et al. (2005). All-optical dynamic correction of distorted communication signals using a photorefractive polymeric hologram. *Applied Physics Letters*, *86*(16), 161103.

Maldonado, J. L., Ponce-de-León, Y., Ramos-Ortíz, G., Rodríguez, M., Meneses-Nava, M. A., Barbosa-García, O., et al. (2009). High diffraction efficiency at low electric field in photorefractive polymers doped with arylimine chromophores. *Journal of Physics D: Applied Physics*, *42*(7), 075102.

Maldonado, J. L., Ramos-Ortiz, G., Meneses-Nava, M. A., Barbosa-García, O., Olmos-López, M., Arias, E., et al. (2007). Effect of doping with C_{60} on

photocurrent and hole mobility in polymer composites measured by using the time-of-flight. *Optical Materials*, *29*(7), 821–826.

Marder, S. R., Kippelen, B., Jen, A. K. Y., & Peyghambarian, N. (1997). Design and synthesis of chromophores and polymers for electro-optic and photorefractive applications. *Nature*, *388*(6645), 845–851.

Meerholz, K., Volodin, B. L., Kippelen, B., & Peyghambarian, N. (1994). A photorefractive polymer with high optical gain and diffraction efficiency near 100%. *Nature*, *371*, 497–500.

Meyer, C. D., Joiner, C. S., & Stoddart, J. F. (2007). Template-directed synthesis employing reversible imine bond formation. *Chemical Society Reviews*, *36*(11), 1705–1723.

Moon, I. K., & Kim, N. (2009). The synthesis, electrochemical and theoretical nonlinear optical properties of push–pull chromophores for photorefractive composites. *Dyes and Pigments*, *82*(3), 322–328.

Moon, I. K., Choi, J., & Kim, N. (2013). High-performance photorefractive composite based on non-conjugated main-chain, hole-transporting polymer. *Macromolecular Chemistry and Physics*, *214*(4), 478–485.

Oh, J. W., Lee, C., & Kim, N. (2009). The effect of trap density on the space charge formation in polymeric photorefractive composites. *Journal of Chemical Physics*, *130*(13), 134909, 1–6.

Ostroverkhova, O., & Moerner, W. E. (2004). Organic photorefractives: Mechanisms, materials, and applications. *Chemical Reviews*, *104*(7), 3267–3314.

Simonov, A. N., Larichev, A. V., Shibaev, V. P., & Stakhanov, A. I. (2001). High-quality correction of wavefront distortions using low-power phase conjugation in azo dye containing LC polymer. *Optics Communications*, *197*(1), 175–185.

Sun, S.-S., & Dalton, L. R. (Eds.). (2008). *Organic and Polymeric Photorefractive Materials and Devices; O. Ostroverkhova, in "Introduction to Organic Electronic and Optoelectronic Materials and Devices"*. (pp. 607–636). FL, USA: Taylor and Francis Group.

Tay, S., Blanche, P. A., Voorakaranam, R., Tunc, A. V., Lin, W., Rokutanda, S., et al. (2008). An updatable holographic three-dimensional display. *Nature*, *451*(7179), 694–698.

Thomas, J., Fuentes-Hernandez, C., Yamamoto, M., Cammack, K., Matsumoto, K., Walker, G. A., et al. (2004). Bistriarylamine polymer-based composites for photorefractive applications. *Advanced Materials*, *16*(22), 2032–2036.

Winiarz, J. G. (2007). Enhancement of the photorefractive response time in a polymeric composite photosensitized with CdTe nanoparticles. *Journal of Physical Chemistry C*, *111*(5), 1904–1911.

Winiarz, J. G., & Ghebremichael, F. (2004). Beam cleanup and image restoration with a photorefractive polymeric composite. *Applied Optics*, *43*(15), 3166–3170.

Würthner, F., Wortmann, R., & Meerholz, K. (2002). Chromophore design for photorefractive organic materials. *ChemPhysChem*, *3*(1), 17–31.

Yeh, P. (1993). *Introduction to photorefractive nonlinear optics*. NY, USA: John Wiley.

Zamiri, S., Reitinger, B., Portenkirchner, E., Berer, T., Font-Sanchis, E., Burgholzer, P., et al. (2014). Laser ultrasonic receivers based on organic photorefractive polymer composites. *Applied Physics B*, *114*(4), 509–515.

Zamiri, S., Reitinger, B., Rodríguez-Rivera, M. A., Ramos-Ortíz, G., Burgholzer, P., Bauer, S., et al. (2015). Employing 532 nm wavelength in a laser ultrasound interferometer based on photorefractive polymer composites. *Open Access Library Journal*, *2*(e1247), 1–6. http://dx.doi.org/10.4236/oalib.1101247

Zhao, Z., Li, Z., Lam, J. W., Maldonado, J. L., Ramos-Ortiz, G., Liu, Y., et al. (2011). High hole mobility of 1,2-bis [4′-(diphenylamino) biphenyl-4-yl]-1,2-diphenylethene in field effect transistor. *Chemical Communications*, *47*(24), 6924–6926.